Kinetics of the Hydrogen Abstraction $C_2H_3^{\bullet}$ + Alkane → C_2H_4 + Alkyl Radical Reaction Class

Marta Muszyńska,[†] Artur Ratkiewicz,[†] Lam K. Huynh,[‡] and Thanh N. Truong*[,‡]

Chemistry Institute, University of Bialystok, Hurtowa 1 15-399 Bialystok, Poland, and Henry Eyring Center for Theoretical Chemistry, Department of Chemistry, University of Utah, 315 South 1400 East Room 2020, Salt Lake City, Utah 84112

Received: April 23, 2009; Revised Manuscript Received: June 3, 2009

This paper presents an application of the reaction class transition state theory (RC-TST) to predict thermal rate constants for hydrogen abstraction reactions of the type C_2H_3 + alkane → C_2H_4 + alkyl radical. The linear energy relationship (LER) was proven to hold for both noncyclic and cyclic hydrocarbons. We have derived all parameters for the RC-TST method from rate constants of 19 representative reactions, coupling with LER and the barrier height grouping (BHG) approach. Both the RC-TST/LER, where only reaction energy is needed, and the RC-TST/BHG, where no other information is needed, can predict rate constants for any reaction in this reaction class with satisfactory accuracy for combustion modeling. Our analysis indicates that less than 90% systematic errors on the average exist in the predicted rate constants using the RC-TST/LER or RC-TST/BHG method, while in comparison to explicit rate calculations, the differences are within a factor of 2 on the average.

1. Introduction

The vinyl radical (C_2H_3) is an important intermediate in combustion processes as well as in low temperature extraterrestrial atmospheres.[1] In combustion, it is a key intermediate arising from the decomposition of higher hydrocarbons in essentially all flames, for example, aliphatic hydrocarbons[2] and/or cyclopentene[3] flames, that plays an important role in molecular weight growth chemistry leading to the production of the first aromatic rings,[4] polycyclic aromatic hydrocarbons, and eventually soot.[5−7] For ethylene flames, for both low and high temperature combustion, the accurate knowledge of the vinyl radicals concentrations is of crucial importance to properly explain the primary effect of partial premixing with oxygen, which manifests itself by decreasing of the maximum concentration of acetylene.[8] Because the title reaction class is an important pathway of decay of the C_2H_3 radicals, accurate rates of reactions in this class are necessary to properly predict the fate of the C_2H_3 species.

Despite the importance of vinyl radical in combustion chemistry, knowledge of its reaction kinetics has been relatively scarce experimentally or theoretically. In general, chemical reactions of unsaturated carbon containing free radicals, such as vinyl, have not been investigated experimentally with the degree of thoroughness that has been associated with studies of saturated alkyl radicals such as CH_3. Moreover, most of available data are provided in a limited temperature range only, whereas for modeling the combustion of hydrocarbon fuels, especially for large hydrocarbons such as kerosene or gasoline, kinetic information for the temperature range from 300 to 2000 K is needed. The reaction class transition state theory (RC-TST) has shown to be a powerful method of filling the gap, with more than 10 papers already published. In this study, we applied the RC-TST method to derive all parameters for estimating the rate constants of any reaction belonging to the alkane + C_2H_3 → alkyl radical + C_2H_4 reaction class. This is done by first deriving analytical correlation expressions for rate constants of the reference reaction with those in a small representative set of the class from explicit direct DFT dynamics calculations of rate constants for all reactions in this representative set. The assumption is that these correlation expressions can be extended to all reactions in the class. So far, this assumption has been shown to be valid.[9−13] To develop RC-TST/linear energy relationship (LER) parameters for the alkane + C_2H_3 → alkyl radical + C_2H_4 reaction class, the representative set consists of 19 reactions as shown in Table 1.

R1 is the reference reaction. Of these, eight reactions are hydrogen abstractions from primary C atom (type p), seven others are from secondary carbon (type s), and the four remaining are hydrogen abstractions of type t. Note that the training set does not contain cyclic hydrocarbons. The validity of the derived LER for cyclic hydrocarbons is used as a test on the extendibility of the RC-TST methodology.

2. Methodology

2.1. RC-TST. Because the details of the RC-TST method have been presented elsewhere,[9,14] we discuss only its main features here. It is based on the realization that reactions in the same class have the same reactive moiety; thus, the difference between the rate constants of any two reactions is mainly due to differences in the interactions between the reactive moiety and their different substituents. Within the RC-TST framework, the rate constant of an arbitrary reaction (denoted as k_a) is proportional to the rate constant of a reference reaction, k_r. Usually, one often would choose the reference reaction to be the smallest reaction in the class, which is referred to as the principal reaction. Any particular reaction in the same class is obtained by extrapolating k_r with a temperature dependent function $f(T)$:

* To whom correspondence should be addressed. E-mail: Thanh.Truong@utah.edu.
[†] University of Bialystok.
[‡] University of Utah.

10.1021/jp903762x CCC: $40.75
Published on Web 07/01/2009

$$k_a(T) = f(T) \times k_r(T) \quad (1)$$

The rate constants for the reference reaction can be calculated accurately from first principles. The key idea of the RC-TST method is to factor $f(T)$ into different components under the TST framework:

$$f(T) = f_\sigma \times f_\kappa \times f_Q \times f_V \quad (2)$$

where f_σ, f_κ, f_Q, and f_V are symmetry number, tunneling, partition function, and potential energy factors, respectively. These factors are simply the ratios of the corresponding components in the TST expression for the two reactions:

$$f_\sigma = \frac{\sigma_a}{\sigma_r} \quad (3)$$

$$f_\kappa(T) = \frac{\kappa_a(T)}{\kappa_r(T)} \quad (4)$$

$$f_Q(T) = \frac{\left(\frac{Q_a^{\neq}(T)}{\Phi_a^R(T)}\right)}{\left(\frac{Q_r^{\neq}(T)}{\Phi_r^R(T)}\right)} = \frac{\left(\frac{Q_a^{\neq}(T)}{Q_r^{\neq}(T)}\right)}{\left(\frac{\Phi_a^R(T)}{\Phi_r^R(T)}\right)} \quad (5)$$

$$f_V(T) = \exp\left[-\frac{(\Delta V_a^{\neq} - \Delta V_r^{\neq})}{k_B T}\right] = \exp\left[-\frac{\Delta\Delta V^{\neq}}{k_B T}\right] \quad (6)$$

where $\kappa(T)$ is the transmission coefficient accounting for the quantum mechanical tunneling effects; σ is the reaction symmetry number; $Q^{\neq}$ and Φ^R are the total partition functions (per unit volume) of the transition state (TS) and reactants, respectively; $\Delta V^{\neq}$ is the classical reaction barrier height; T is the temperature in Kelvin; and k_B and h are the Boltzmann and Planck constants, respectively. The potential energy factor can be calculated using the reaction barrier heights of the arbitrary reaction and the reference reaction. The classical reaction barrier height $\Delta V^{\neq}$ for the arbitrary reaction can be obtained using the LER, similar to the well-known Evans−Polanyi linear free energy relationship, between classical barrier heights and reaction energies of reactions in a given reaction class without having to calculate them explicitly. It is worth mentioning that within the RC-TST framework, the recrossing effect is only implicitly included in the rate constants of the reference reaction and is not explicitly included in the calculation of the reaction class factors.

2.2. Computational Details. All of the electronic structure calculations were carried out using the Gaussian 03 suite of programs.[15] A hybrid nonlocal density functional theory (DFT), particularly Becke's half and half[16] (BH&H) nonlocal exchange and Lee−Yang−Parr[17] (LYP) nonlocal correlation functionals, has been found previously to be sufficiently accurate for predicting the TS properties.[18,19] Note that within the RC-TST framework, as discussed above, only the relative barrier heights are needed. Our previous studies have shown that the relative barrier heights can be accurately predicted by the BH&HLYP method.[11−13] Geometries of reactants, TSs, and products were optimized at the BH&HLYP level of theory with the Dunning's correlation-consistent polarized valence double-ζ basis set [3*s*2*p*1*d*/2*s*1*p*] denoted as cc-pVDZ, which is sufficient to capture the physical change along the reaction coordinate for this type of reaction. Each stationary point was characterized via vibrational frequency calculations using the same theoretical method and basis set from which the geometry was generated. This information was used to derive the RC-TST factors. The AM1 semiempirical method was also employed to calculate the reaction energies of those reactions considered here. AM1 and BH&HLYP/cc-pVDZ reaction energies were then used to derive the LER's between the barrier heights and the reaction energies. Note that AM1 reaction energy is only used to extract an accurate barrier height from the LERs, it does not directly involve any rate calculations.

Minima were confirmed to have adequate convergence and zero imaginary vibrational frequencies. The TS structure was confirmed to have one imaginary vibrational frequency and furthermore shown to be connected to the desired reactant and product by displacement along the normal coordinate for the imaginary vibrational frequency in the positive and negative directions. For the sake of comparison, we employed the Gaussian-3 approach to calculate stationary points at a higher, more accurate level of theory. The G3//B3LYP (or G3B3) basis set extrapolation method uses B3LYP/6-31G(d) geometries for

TABLE 1

(R_1)	$CH_3CH_3 + C_2H_3$	→	$CH_2{\cdot}CH_3 + C_2H_4$
(R_2)	$CH_3CH_2CH_3 + C_2H_3$	→	$CH_2{\cdot}CH_2CH_3 + C_2H_4$
(R_3)	$CH_3CH_2CH_3 + C_2H_3$	→	$CH_3CH{\cdot}CH_3 + C_2H_4$
(R_4)	$CH_3CH_2CH_2CH_3 + C_2H_3$	→	$CH_2{\cdot}CH_2CH_2CH_3 + C_2H_4$
(R_5)	$CH_3CH_2CH_2CH_3 + C_2H_3$	→	$CH_3CH{\cdot}CH_2CH_3 + C_2H_4$
(R_6)	$CH_3CH_2CH_2CH_2CH_3 + C_2H_3$	→	$CH_2{\cdot}CH_2CH_2CH_2CH_3 + C_2H_4$
(R_7)	$CH_3CH_2CH_2CH_2CH_3 + C_2H_3$	→	$CH_3CH{\cdot}CH_2CH_2CH_3 + C_2H_4$
(R_8)	$CH_3CH_2CH_2CH_2CH_3 + C_2H_3$	→	$CH_3CH_2CH{\cdot}CH_2CH_3 + C_2H_4$
(R_9)	$CH_3CH_2CH_2CH_2CH_2CH_3 + C_2H_3$	→	$CH_2{\cdot}CH_2CH_2CH_2CH_2CH_3 + C_2H_4$
(R_{10})	$CH_3CH_2CH_2CH_2CH_2CH_3 + C_2H_3$	→	$CH_3CH{\cdot}CH_2CH_2CH_2CH_3 + C_2H_4$
(R_{11})	$CH_3CH_2CH_2CH_2CH_2CH_3 + C_2H_3$	→	$CH_3CH_2CH{\cdot}CH_2CH_2CH_3 + C_2H_4$
(R_{12})	$(CH_3)_2CHCH_2CH_2CH_3 + C_2H_3$	→	$(CH_3)_2C{\cdot}CH_2CH_2CH_3 + C_2H_4$
(R_{13})	$(CH_3)_2CHCH(CH_3)CH_3 + C_2H_3$	→	$(CH_3)_2C{\cdot}CH(CH_3)CH_3 + C_2H_4$
(R_{14})	$CH_3CH_2CH_2CH_2CH_2CH_2CH_3 + C_2H_3$	→	$CH_2{\cdot}CH_2CH_2CH_2CH_2CH_2CH_3 + C_2H_4$
(R_{15})	$CH_3CH_2CH_2CH_2CH_2CH_2CH_3 + C_2H_3$	→	$CH_3CH{\cdot}CH_2CH_2CH_2CH_2CH_3 + C_2H_4$
(R_{16})	$CH_3CH_2CH_2CH_2CH_2CH_2CH_2CH_3 + C_2H_3$	→	$CH_2{\cdot}CH_2CH_2CH_2CH_2CH_2CH_2CH_3 + C_2H_4$
(R_{17})	$(CH_3)_2CHCH(CH_3)CH_2CH_3 + C_2H_3$	→	$(CH_3)_2C{\cdot}CH(CH_3)CH_2CH_3 + C_2H_4$
(R_{18})	$(CH_3)_2CHCH(CH_3)CH_2CH_3 + C_2H_3$	→	$(CH_3)_2CHC{\cdot}(CH_3)CH_2CH_3 + C_2H_4$
(R_{19})	$CH_3CH_2CH_2CH_2CH_2CH_2CH_2CH_2CH_3 + C_2H_3$	→	$CH_2{\cdot}CH_2CH_2CH_2CH_2CH_2CH_2CH_2CH_3 + C_2H_4$

the single-point energy calculations at the higher levels of theory instead of MP2/ 6-31G(d) geometries as used in G3 and G3(MP2).

To derive the RC-TST correlation functions, TST/Eckart rate constants for all reactions in the above representative reaction set were calculated employing the kinetic module of the web-based Computational Science and Engineering Online (CSE-Online) environment.[20] In these calculations, overall rotations were treated classically, and vibrations were treated quantum mechanically within the harmonic approximation except for the modes corresponding to the internal rotations of the CH_2 and CH_3 groups, which were treated as the hindered rotations (HRs) using the method suggested by Ayala et. al.[21] Thermal rate constants were calculated for the temperature range of 300−3000 K, which is sufficient for many combustion applications such as premixed flame and shock-tube simulations.

3. Results and Discussion

In the section below, we first report on the stationary points and rate constants for the reference reaction, and then, we describe how the RC-TST factors are derived using the representative reaction set. Subsequently, we perform three error analyses to provide some estimates of the accuracy of the RC-TST method applied to this reaction class. The first error analysis is the direct comparison between the calculated rate constants and those available in the literature for reactions R_2 and R_3. The second error analysis is the comparison between the rate constants for reactions R_2−R_{19} calculated using the RC-TST method and those obtained using the explicit full TST/Eckart method. The final analysis is on the systematic errors caused by introducing approximations in the RC-TST correlation functions.

3.1. Potential Energy Surfaces. The optimized geometrical parameters of the reactants and the TS of the C_2H_6 + C_2H_3 reaction at the BH&HLYP/cc-pVDZ and QCISD/cc-pVDZ levels of theory are shown in Figure 1. The TS was confirmed by normal-mode analysis to have only one imaginary frequency whose mode corresponds to the transfer of the hydrogen atom between C_2H_6 and C_2H_3 structures. From Figure 1, it is seen that the BH&HLYP/cc-pVDZ method gives optimized geometries close to those from the QCISD/cc-pVDZ level of theory for the reactants and TS with the largest difference of 0.024 Å for double CC bond in the vinyl radical. For the frequency calculation, the results from BH&HLYP/cc-pVDZ are consistent with QCISD/cc-pVDZ level with the average absolute difference of about 32 cm^{-1}. This leads to the differences in the total zero-point energies of 1.49, 1.59, and 1.57 kcal/mol for reactant, TS, and product, respectively. Consequently, the differences between the two levels on the zero-point energy corrections on the classical barrier and reaction energy are insignificant, that is, less than 0.2 kcal/mol. The zero-point energy-corrected barrier height calculated at various levels of theory is listed in Table 2. Consistent with our previous work,[9,10,12,13] the BH&HLYP/cc-pVDZ method gives rather accurate results for TS properties comparable to more accurate correlation methods, like CCSD(T). The most accurate method considered here is the compound CBS-QB3 method, which predicts the barrier height and reaction energy to be 8.5 and −9.2 kcal/mol, respectively. It is interesting to note that all of the methods listed in Table 2, except B3LYP, predict the barrier height between 8 and 10 kcal/mol and the reaction energy between −9 and −11 kcal/mol. B3LYP performs poorly as this method underestimates the barrier height by 2.3 kcal/mol. Because of the spin contamination, a larger error in reaction energy is observed for the MPn methods. It is interesting to note that the CCSD(T)/cc-pVDZ//BH&HLYP/cc-pVDZ results for both reaction energy and barrier height are in excellent agreement with the CBQ-QB3 values with the differences less than 0.5 kcal/mol. Thus, we can use the CCSD(T)/cc-pVDZ//BH&HLYP/cc-pVDZ method to establish the reliability of the BH&HLYP calculated barriers for H abstractions from secondary ($CH_3CH_2CH_3$ + C_2H_3 → $CH_3CH^{\bullet}CH_3$ + C_2H_4 reaction) and tertiary ($CH_3CH_2CH_3$ + C_2H_3 → $CH_3CH^{\bullet}CH_3$ + C_2H_4 reaction) C atoms. Results shown

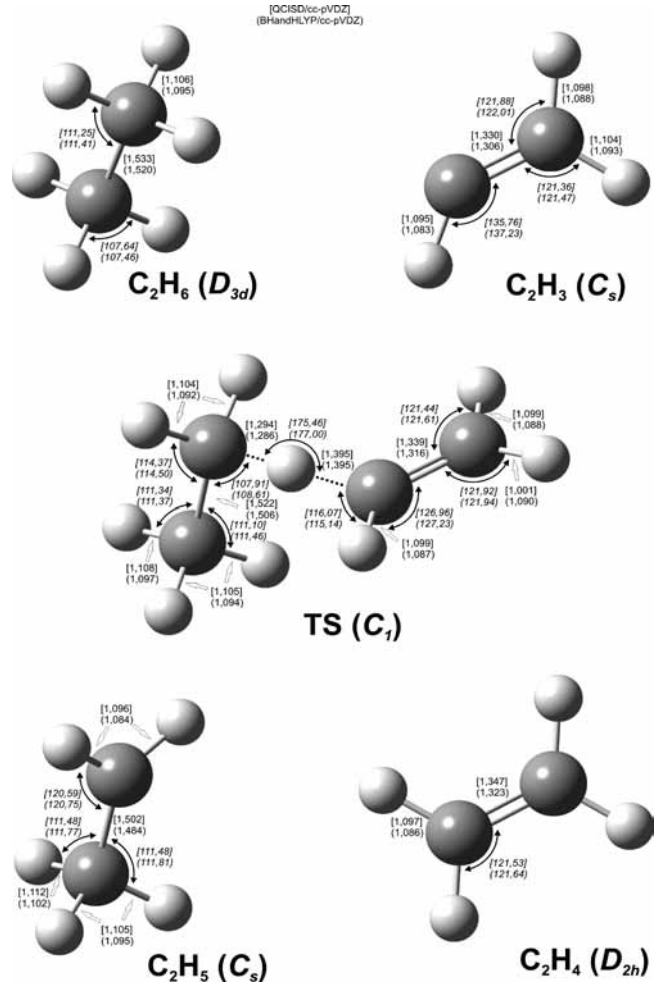

Figure 1. Optimized geometries (distances in Å and angles in degrees) of the reactants C_2H_6 and C_2H_3, products C_2H_6 and C_2H_4, and TS at the BH&HLYP/cc-pVDZ and QCISD/cc- pVDZ (square brackets) levels of theory. Angle values are marked as italics.

TABLE 2: Calculated Barrier Height and Reaction Energy for the C_2H_6 + C_2H_3 Reaction (Numbers Are in kcal/mol)[a]

level of theory	ΔE	$\Delta V^{\neq}$
B3LYP/cc-pVDZ	−9.6	6
B3LYP/cc-pVTZ	−9.9	7.8
BH&HLYP/cc-pVDZ	−10.2	9.7
BH&HLYP/cc-pVTZ	−10.5	9.1
CCSD(T)/cc-pVDZ //BH&HLYP/cc-pVDZ	−9.1	9.0
QCISD/cc-pVDZ// BH&HLYP/cc-pVDZ	−9.1	10.0
MP2/cc-pVDZ// BH&HLYP/cc-pVDZ	−14.1	9.8
MP2/cc-pVTZ// BH&HLYP/cc-pVDZ	−16.4	9.7
MP4/cc-pVDZ// BH&HLYP/cc-pVDZ	−13.1	9.4
MP4/cc-pVTZ// BH&HLYP/cc-pVDZ	−13.9	9.2
CBS-QB3	−9.2	8.5
G2/MP2(full)/6-31+G(d)[27]		9.7
G2//QCISD/6-31G(d,p)[27]		9.2

[a] The zero-point energy correction is included.

TABLE 3: Calculated Barrier Height and Reaction Energy for the $CH_3CH_2CH_3 + C_2H_3 \rightarrow CH_3CH\cdot CH_3 + C_2H_4$ and $CH_3CH(CH_3)CH_3 + C_2H_3 \rightarrow CH_3C\cdot(CH_3)CH_3 + C_2H_4$ Reactions (Numbers Are in kcal/mol)[a]

reaction	level of theory	ΔE	$\Delta V^{\neq}$
$CH_3CH_2CH_3 + C_2H_3 \rightarrow CH_3CH\cdot CH_3 + C_2H_4$	BH&HLYP/cc-pVDZ	−13.4	7.9
	CCSD(T)/cc-pVDZ //BH&HLYP/cc-pVDZ	−11.5	9.0
$CH_3CH(CH_3)CH_3 + C_2H_3 \rightarrow CH_3C\cdot(CH_3)CH_3 + C_2H_4$	BH&HLYP/cc-pVDZ	−15.8	6.5
	CCSD(T)/cc-pVDZ //BH&HLYP/cc-pVDZ	−13.8	5.1

[a] The zero-point energy correction is included.

in Table 3 further confirm the accuracy of the BH&HLYP for calculating TS properties of reactions at different carbon sites.

3.2. Rate Constants of the Reference Reaction. The first task for using the RC-TST method is determination of thermal rate constants of the reference reaction. In our previous studies,[9,10,12,14,22] we suggested the use of the smallest reaction, that is, the principal reaction of the class, to be the reference reaction since its rate constants can be calculated accurately from first principles or are often known experimentally. However, we found that the principal reaction is not always the best reference reaction, and it is also true here.[12] In fact, the hydrogen abstraction by vinyl radical from ethane, $C_2H_3 + C_2H_6$, is a better reference reaction than the principal $C_2H_3 + CH_4$ reaction for the following reasons. Although methane is the simplest hydrocarbon, it is known to have strange behavior as compared to other saturated hydrocarbons. Because of its lack of a C−C bond, which exists in larger hydrocarbons, the reaction barrier of reaction $C_2H_3 + CH_4$ is appreciably larger by at least about 3 kcal/mol than those of other reactions in the class, as discussed later. In addition, on the basis of our analyses of both reactions of C_2H_3 with methane and ethane, it is shown that the $C_2H_3 + C_2H_6$ reaction gives a better correlation than the $C_2H_3 + CH_4$ reaction, especially for vibrational partition function factors. For these reasons, the further discussion is based on the use of the reaction between vinyl and ethane as the reference reaction.

Experimental kinetic data from direct measurements for the reference reaction are available in the NIST[23] database. Hidaka et al.[24] studied the thermal decomposition of ethane behind reflected shock waves over the temperature range 1200−1700 K and over the pressure range 1.7−2.5 atm. In addition, rate constants of the $C_2H_3 + C_2H_6 \rightarrow C_2H_4 + C_2H_5$ reaction were derived from fitting to a complex mechanism. Stiller et al.[25] estimated this rate with BEBO method for temperatures 480, 500, and 520 K. Rate constants suggested from a review by Tsang and Hampson,[26] in the high temperature regime ($T > 1000$ K), agree well with the most recent theoretical calculations presented by Liu et al.[27] These authors calculated thermal rate constants using the canonical variational TS theory (CVT) and the small-curvature tunneling correction (SCT). The energetic data were obtained at the G2 level of theory together with the gradient and Hessian information at QCISD(T)/6-31+G(d). These rate constants are valid over a wide range of temperatures from 200 to 3000 K. These rate constants are sufficiently accurate for the application of the RC-TST/LER method and thus are used here. They can be fitted to the Arrhenius equation as:

$$k(T) = 1.78075 \times 10^{-26} \times T^{4.492163} \times \exp\left(\frac{-2502.58}{T}\right) (\mathrm{cm^3\ s^{-1}\ molecule^{-1}}) \quad (7)$$

Figure 2 reports the rate constants available in the literature for this reaction obtained by experiments and simulations.

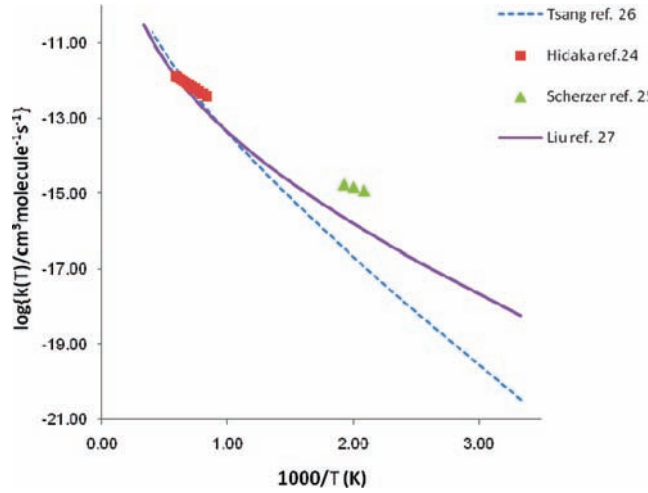

Figure 2. Arrhenius plots of the calculated and available rate constants for the $C_2H_6 + C_2H_3 \rightarrow C_2H_5 + C_2H_4$ reaction in the temperature range of 300−3000 K.

3.3. Reaction Class Parameters. This section describes how the RC-TST factors were derived using the representative reaction set.

3.3.1. Potential Energy Factor. The potential energy factor can be calculated using eq 6, where $\Delta V_a^{\neq}$ and $\Delta V_r^{\neq}$ are the barrier heights of the arbitrary and reference reactions, respectively. It has been shown previously that within a given class, there is a LER between the barrier height and the reaction energy, similar to the well-known Evans−Polanyi linear free energy relationship. Thus, with a LER, accurate barrier heights can be predicted from only the reaction energies. In this study, the LER is determined, where the reaction energy can be calculated by either the AM1 or the BH&HLYP level of theory. Alternatively, it is possible to approximate all reactions at the same type of carbon atom site as having the same barrier height, namely, the average value. In previous studies,[12] this approximation was referred to as the barrier height grouping (BHG) approximation. It was shown that substitution of an alkyl group will stabilize the radical species, thus lowering the barrier height. Thus, one can expect hydrogen abstractions reactions from the tertiary carbon to have lower barrier height than those from a secondary carbon. The same relationship is expected to hold between H abstractions from a secondary and primary carbon atom. These expectations were confirmed in our DFT calculation, when the average scaled barrier heights for H-shift from a primary, secondary, and tertiary carbon were 11.74, 10.04, and 8.84 kcal/mol, respectively. The reaction energies and barrier heights for all representative reactions in the representative set are given explicitly in Table 4.

The observed LERs plotted against the reaction energies calculated at the BH&HLYP/cc-pVDZ and AM1 levels are shown in Figure 3a,b, respectively. These linear fits were obtained using the least-squares fitting method and have the following expressions:

$$\Delta V_a = 0.4428 \times \Delta E^{BH\&HLYP} + 15.724 \text{ (kcal/mol)} \quad (8a)$$

$$\Delta V_a = 0.2951 \times \Delta E^{AM1} + 14.862 \text{ (kcal/mol)} \quad (8b)$$

Except for the reference reaction, the absolute deviations of reaction barrier heights between the LERs and the direct DFT BH&HLYP/cc-pVDZ calculations are smaller than 0.37 kcal/mol (see Table 4). The mean absolute deviation of reaction barrier heights predicted from BH&HLYP and AM1 reaction energies are 0.09 and 0.24 kcal/mol, respectively. These deviations are, in fact, smaller than the systematic errors of the computed reaction barriers from full electronic structure calculations (see Tables 2 and 3). This is certainly acceptable for kinetic modeling. It should be noted that at this point, only the relative barrier height is needed. To compute these relative values, the barrier height of the reference reaction R_1 calculated at the same level of theory, that is, BH&HLYP/cc-pVDZ, is needed and has the value of 11.54 kcal/mol (see Table 4). To test the extendibility of the LER equations to reactions with other alkanes not in the training set such as cycloalkanes, we used three reactions, namely, cyclobutane + C_2H_3, cyclopentane + C_2H_3, and cyclohexane + C_2H_3. From Table 4, for the BH&HLYP LER, the unsigned errors in the barrier heights for the three reactions are 0.26, 0.40, and 0.16 kcal/mol, respectively, which gives a mean absolute deviation 0.27 kcal/mol. Consequently, the formula (eq 8a) is also applicable to all alkanes. However, we found AM1-based LER (eq 8b) cannot be extended to cycloalkanes.

For the BHG approach, the average scaled barrier heights are assigned to all reactions in the same type of carbon site, namely, 11.74, 10.04, and 8.84 kcal/mol for the primary, secondary, and tertiary carbon sites. The averaged deviations are 0.37, 0.20, and 0.53 kcal/mol, respectively, which correspond to 0.4, 1.8 and 4.9% of the mean barrier heights. Therefore, this approach can also be used to estimate the relative barrier height with less than 5% deviation. The key advantage of this approach is that it does not require any additional information to estimate rate constants.

In conclusion, the barrier heights for any reaction in this reaction class can be obtained by using either the LER or the BHG approach. The estimated barrier height is then used to calculate the potential energy factor using eq 6. The performance for such estimations on the whole representative reaction set is discussed in the error analyses below.

3.3.2. Reaction Symmetry Number Factor. The reaction symmetry number factors f_σ were calculated simply from the ratio of reaction symmetry numbers of the arbitrary and reference reactions using eq 3 and are listed in Table 5. The reaction symmetry number of a reaction is given by the number of symmetrically equivalent reaction paths. For the title reaction class, this number is the product of the number of H atoms connected to the hydrogen abstraction site (three for primary carbons, two for secondary, and one for tertiary) and the number of equivalent abstraction sites in the molecule. The reference reaction (#1 in the training set) can serve as a useful example here. Because there are two equivalent primary C atoms in the CH_3CH_3 molecule, the reaction symmetry number is equal to $2 \times 3 = 6$. In any case, this number can be easily calculated from the molecular topology of the reactant; thus, the symmetry number factor can be calculated exactly.

3.3.3. Tunneling Factor. The tunneling factor f_κ is the ratio of the transmission coefficient of reaction R_a to that of the

TABLE 4: Classical Reaction Energies, Barrier Heights, and Absolute Deviations between Calculated Barrier Heights from DFT and Semiempirical Calculations and Those from LER Expressions and BHG Approach[a]

	ΔE		$\Delta V^{\neq}$				$\lvert\Delta V^{\neq} - \Delta V^{\neq}_{estimated}\rvert$[g]		
reaction	DFT[b]	AM1[c]	DFT[b]	DFT[d]	AM1[e]	BHG[f]	DFT[d]	AM1[e]	BHG[f]
R_1	−9.54	−11.09	11.54	11.50	11.59	11.74	0.04	0.05	0.20
R_2	−8.93	−10.95	11.76	11.77	11.63	11.74	0.01	0.13	0.02
R_3	−12.82	−16.36	9.97	10.05	10.04	10.04	0.07	0.06	0.07
R_4	−9.02	−10.97	11.75	11.73	11.62	11.74	0.02	0.12	0.01
R_5	−12.60	−15.14	10.02	10.14	10.39	10.04	0.12	0.37	0.02
R_6	−9.02	−10.97	11.77	11.73	11.63	11.74	0.04	0.15	0.03
R_7	−12.65	−15.15	10.03	10.12	10.39	10.04	0.09	0.36	0.01
R_8	−12.41	−15.76	10.12	10.23	10.21	10.04	0.11	0.09	0.07
R_9	−9.01	−10.97	11.78	11.73	11.63	11.74	0.05	0.16	0.04
R_{10}	−12.65	−15.14	10.02	10.12	10.39	10.04	0.10	0.37	0.02
R_{11}	−12.46	−15.79	10.10	10.21	10.20	10.04	0.10	0.10	0.06
R_{12}	−15.17	−20.57	9.24	9.01	8.79	8.84	0.24	0.45	0.41
R_{13}	−14.90	−20.89	9.50	9.13	8.70	8.84	0.37	0.80	0.66
R_{14}	−9.02	−10.96	11.78	11.73	11.63	11.74	0.05	0.16	0.04
R_{15}	−12.64	−15.14	10.02	10.13	10.39	10.04	0.10	0.37	0.02
R_{16}	−9.02	−10.96	11.77	11.73	11.63	11.74	0.04	0.14	0.03
R_{17}	−16.76	−21.72	8.19	8.30	8.45	8.84	0.11	0.26	0.64
R_{18}	−16.43	−21.18	8.42	8.45	8.61	8.84	0.03	0.20	0.42
R_{19}	−8.99	−10.96	11.77	11.74	11.63	11.74	0.03	0.14	0.03
C4[h]	−12.46		9.95	10.21			0.26		
C5[h]	−15.35		9.32	8.93			0.40		
C6[h]	−12.40		10.39	10.23			0.16		
MAD[i]						0.09	0.24	0.15	

[a] The zero-point energy correction is not included. Energies are in kcal/mol. [b] Calculated at the BH&HLYP/cc-pVDZ level of theory. [c] Calculated at the AM1 level of theory. [d] Calculated from the LER using reaction energies calculated at the BH&HLYP/cc-pVDZ level of theory: eq 9a. [e] Calculated from the LER using reaction energies calculated at the AM1 level of theory: eq 9b. [f] Estimated from BHG. [g] $\Delta V^{\neq}$ from BH&HLYP/cc-pVDZ calculations; $\Delta V^{\neq}_{estimated}$ from the LER using BH&HLYP/cc-pVDZ and AM1 reaction energies or from BHG. [h] C4, cyclobutane + C_2H_3; C5, cyclopentane + C_2H_3; and C6, cyclohexane + C_2H_3; reactions not in the training set. [i] Mean absolute deviations (MAD) for reactions R_2−R_{19}.

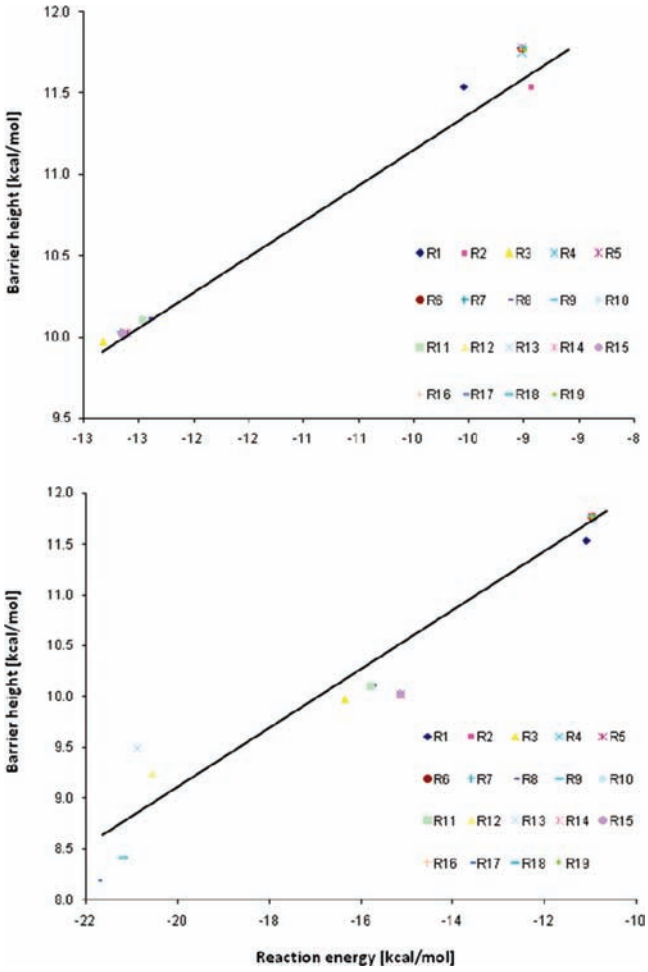

Figure 3. LER plot of the barrier heights, $\Delta V^{\neq}$, vs the reaction energies, ΔE. Barrier heights were calculated at the BH&HLYP/cc-pVDZ level of theory. ΔE values were calculated at (a) BH&HLYP/cc-pVDZ and (b) AM1 levels of theory.

reference reaction R_r. Because of cancellation of errors in calculations of the tunneling factors, we have shown[9] that the factor f_κ can be reasonably estimated using the one-dimension Eckart method. Calculated results for the representative reaction set can then be fitted to an analytical expression. It is known that the tunneling coefficient depends on the barrier height. We have shown that the barrier heights group together into three groups, namely, primary, secondary, and tertiary carbon site (see the Potential Energy Factor section); it is expected that reactions in the same group have similar tunneling factors, and thus, the average value can be used for the whole group. Simple expressions for the three tunneling factors for primary, secondary, and tertiary carbon sites are obtained by fitting to the average calculated values and are given below:

$$f_\kappa^{\mathrm{I}} = 1 \text{ for primary carbon sites} \quad (9a)$$

$$f_\kappa^{\mathrm{II}} = 0.983948 - 3.06142 \times \exp(-T/159.4091) \text{ for secondary carbon sites} \quad (9b)$$

$$f_\kappa^{\mathrm{III}} = 0.9722 - 2.60157 \times \exp(-T/204.5322) \text{ for tertiary carbon sites} \quad (9c)$$

The three equations are plotted in Figure 4, and the error analysis at 300 K is listed in Table 5. It can be seen that the same tunneling factor expression can be reasonably assigned to all reactions at the same site with the largest percentage deviation of 43.4% for R_{17} and the mean absolute deviation of 9%, as compared to the direct Eckart calculations. At higher temperatures, tunneling contributions to the rate constants decrease, and thus, as expected, the differences between the approximated values and the explicitly calculated ones also decrease; for example, the maximum error for all reactions is less than 5% at 500 K and 0.1% at 1000 K.

TABLE 5: Calculated Symmetry Number Factors and Tunneling Factors at 300 K

reaction	symmetry number factor	tunneling ratio factor, f_κ			
		Eckart[a]	fitting[b]	deviation[c]	% deviation[d]
R_1	1.00	(45.7)[f]			
R_2	1.00	1.08	1.00	0.08	7.2
R_3	0.33	0.48	0.52	0.04	7.4
R_4	1.00	1.06	1.00	0.06	5.6
R_5	0.67	0.50	0.52	0.02	4.0
R_6	1.00	1.04	1.00	0.04	4.2
R_7	0.67	0.49	0.52	0.03	5.1
R_7	0.33	0.52	0.52	0.00	0.2
R_9	1.00	1.04	1.00	0.04	4.1
R_{10}	1.00	0.55	0.52	0.03	5.8
R_{11}	1.00	0.52	0.52	0.00	0.5
R_{12}	0.17	0.32	0.37	0.05	14.4
R_{13}	0.17	0.49	0.37	0.12	24.5
R_{14}	1.00	1.03	1.00	0.03	3.3
R_{15}	1.00	0.49	0.52	0.03	6.2
R_{16}	1.00	0.83	1.00	0.17	19.9
R_{17}	0.17	0.26	0.37	0.11	43.4
R_{18}	0.17	0.35	0.37	0.02	6.0
R_{19}	1.00	0.99	1.00	0.01	0.6
MAD[e]				0.08	7.2

[a] Calculated directly using Eckart method with BH&HLYP/cc-pVDZ reaction barrier heights and energies. [b] Calculated by using a fitting expression. [c] Absolute deviation between the fitting and the directly calculated values. [d] Percentage deviation (%). [e] Mean absolute deviations (MAD) and deviation percentage between the fitting and the directly calculated values. [f] Tunneling coefficient calculated for reaction R_1 using the Eckart method with the energetic and frequency information at BH&HLYP/cc-pVDZ.

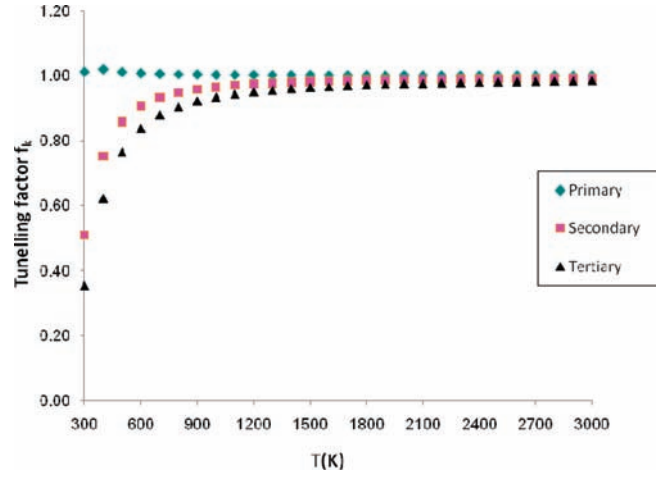

Figure 4. Plots of the tunneling ratio factors f_κ as functions of the temperature for the H abstraction by C_2H_3 from primary, secondary, and tertiary carbon sites in the temperature range of 300−3000 K.

3.3.4. Partition Function Factor. The partition factor is the product of the translational, rotational, internal rotation, vibrational, and electronic component. The translational and rotational factors are temperature-independent. As pointed out in our

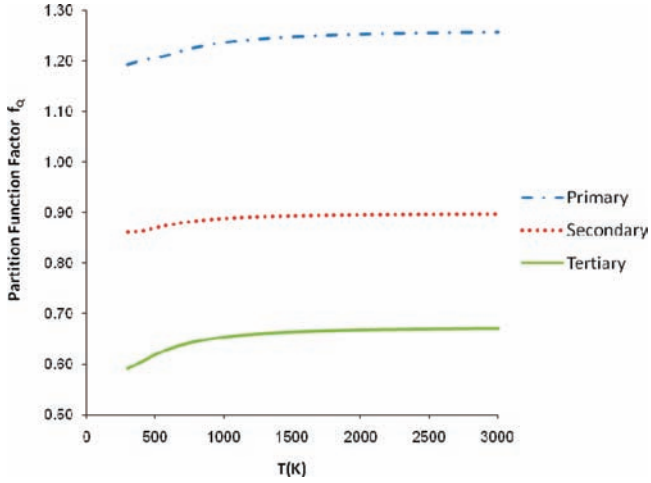

Figure 5. Plots of the average values of the partition function factors for primary, secondary, and tertiary carbon abstraction sites in the temperature range of 300−3000 K.

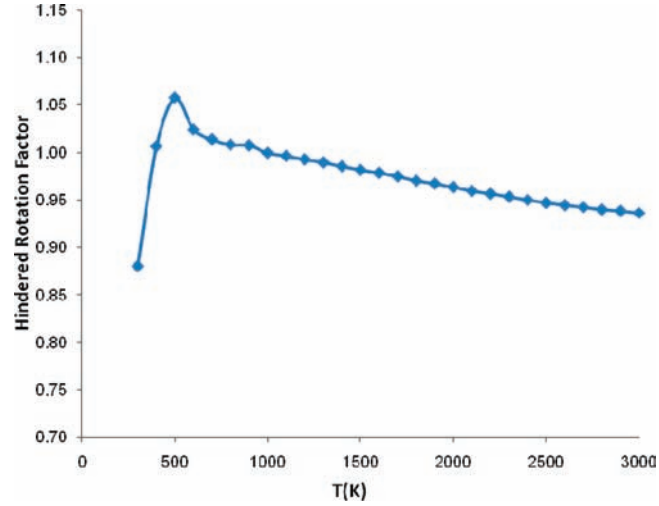

Figure 6. Plot of the average HR corrections to the total rate constants for all reactions in the temperature range of 300−3000 K.

previous study,[12] the temperature-dependent part of the total partition function factor f_Q mainly originates from the differences in the coupling between the substituents with the reactive moiety and its temperature dependence, which arises from the vibrational component and internal rotations only. Note that because contributions from the HR modes are treated separately, they are not included in these partition function calculations. Because the variations in factors corresponding to different types of carbon atom sites were found to be rather significant, we derived different formulas for H abstraction from primary, secondary, and tertiary carbon atoms separately. The average values of partition function factors for primary, secondary, and tertiary carbon abstraction sites, calculated in the temperature range of 300−3000 K, are given in Figure 5. These average values were fitted into analytical expressions as given below:

$$f_Q^{\mathrm{I}} = 1.25386 - 0.11308 \times \exp(-T/546.626) \text{ for primary carbon sites} \quad (10a)$$

$$f_Q^{\mathrm{II}} = 0.88 \text{ for secondary carbon sites} \quad (10b)$$

$$f_Q^{\mathrm{III}} = 0.67059 - 0.15717 \times \exp(-T/458.803) \text{ for tertiary carbon sites} \quad (10c)$$

As one may see from Figure 5, the average value of partition function factor differs from unity. As mentioned earlier, the coupling between substituents with the reactive moiety is believed to account for these differences.

3.3.5. HR Factor. For this reaction class, rotations of the alkyl (for example CH_3) or alkanyl (CH_2) groups along the C−C bond for some reactants, TSs, and products need to be treated as hindered rotors. We used the approach proposed by Ayala et al.[21] The reaction class factor due to these hindered rotors is a measure of the substituent effects on the rate constants from these hindered rotors, relative to that of the reference reaction. The effect of the HR treatment to total rate constants can be seen in Figure 6. For the sake of simplicity and clarity, only the average factor for the whole reaction class is presented. It can be seen from Figure 6 that the HR correction factors are dependent on the temperature. The average value, at $T = 300$ K, is smaller than 1, whereas for other temperatures, the average factor is close to unity. The average value, as applied to the whole class, is fitted into a quadratic expression for 300 K ≤ T ≤ 600 K and as a linear expression for T > 600 K, as given below:

$$f_{\mathrm{HR}} = \begin{cases} -4 \times 10^{-6}T^2 + 0.0041T + 0.0171 & 300 \text{ K} \le T \le 600 \text{ K} \\ 1.040509 - 3.07 \times 10^{-5}T & T > 600 \text{ K} \end{cases} \quad (11)$$

3.4. Prediction of Rate Constants. What we have established so far are the necessary parameters—namely, potential energy factor, reaction symmetry number factor, tunneling factor, and partition function factor—for application of the RC-TST theory to predict rate constants for any reaction in the hydrogen abstraction by the vinyl radical reaction class. The procedure for calculating rate constants of an arbitrary reaction in this class is (i) calculate the potential energy factor using eq 6 with the $\Delta V_{\mathrm{r}}^{\neq}$ value of 11.54 kcal/mol. The reaction barrier height can be obtained using the LER approach by employing eq 8a for BH&HLYP/cc-pVDZ or eq 8b for AM1 reaction energies or by the BHG approach; (ii) calculate the symmetry number factor from eq 3 or see Table 5; (iii) compute the tunneling factor using eq 9a, 9b, or 9c for primary, secondary, and tertiary carbon sites, respectively; (iv) evaluate the partition function factor using eq 10a; (v) evaluate the HR factor using eq 11; and (vi) the rate constants of the arbitrary reaction can be calculated by taking the product of the reference reaction rate constant given by eq 7 with the reaction class factors above. Table 6 summarizes the RC-TST parameters for this reaction class. Rules presented in this table enable one to obtain any rate constants within the hydrogen abstraction by vinyl radical reaction class. For the reasons discussed in section 3.2, these rules should not be used for the simplest reaction within this class, namely, $CH_4 + C_2H_3 \rightarrow CH_3 + C_2H_4$. For this reaction, we recommend using rate constants obtained by Liu et al.,[27] namely:

$$k_{(CH_4+C_2H_3\rightarrow CH_3+C_2H_4)}(T) = 6.77 \times 10^{-30} \times T^{5.456595} \times \exp\left(\frac{2822.724057}{T}\right) (\mathrm{cm^3\ s^{-1}\ molecule^{-1}}) \quad (12)$$

TABLE 6: Parameters and Formulations of the RC-TST Method for the Hydrogen Abstraction from Alkanes by Vinyl Radical Reaction Class ($C_2H_3 + C_2H_6 \rightarrow C_2H_4 + C_2H_5$ Is the Reference Reaction)

	$k_a(T) = k_p(T) \times f_k(T) \times f_Q(T) \times f_{HR}(T) \times f_v(T) \times f_\sigma$; $f_v(T) = \exp[(-(\Delta V^{\neq} - \Delta V_r^{\neq}))/(k_B T)]$	
	T is in Kelvin; $\Delta V^{\neq}$ and ΔE are in kcal/mol; the zero-point energy correction is not included	
f_σ	calculated explicitly from the symmetry of reactions (see Table *4*)	
$f_k(T)$	$f_k^{I} = 1$	for primary carbon sites
	$f_k^{II} = 0.983948 - 3.06142 \times \exp(-T/159.4091)$	for secondary carbon sites
	$f_k^{III} = 0.9722 - 2.60157 \times \exp(-T/204.5322)$	for tertiary carbon sites
$f_Q(T)$	$f_Q^{I} = 1.25386 - 0.11308 \times \exp(-T/546.626)$	for primary carbon sites
	$f_Q^{II} = 0.88$	for secondary carbon sites
	$f_Q^{III} = 0.67059 - 0.15717 \times \exp(-T/458.803)$	for tertiary carbon sites
$f_{HR}(T)$	$f_{HR} = \begin{cases} -4 \times 10^{-6} T^2 + 0.0041T + 0.0171 & 300\ \text{K} \le T \le 600\ \text{K} \\ 1.040509 - 3.07 \times 10^{-5} T & T > 600\ \text{K} \end{cases}$	
$\Delta V^{\neq}$	$\Delta V_a = 0.4428 \times \Delta E^{BH\&HLYP} + 15.724$	
	$\Delta V_a = 0.2951 \times \Delta E^{AM1} + 14.862$	
	$\Delta V_r^{\neq} = 11.54$ kcal/mol	
$k_r(T)$	$k_r(T) = 1.78075 \times 10^{-26} \times T^{4.492163} \times \exp(-2502.58/T)$	(cm^3 $molecule^{-1}$ s^{-1})
BHG approach	$k(T) = 2.1369 \times 10^{-26} \times T^{4.4983} \times \exp(-2613.9911/T)$	for primary carbon sites
	$k(T) = 7.74811 \times 10^{-26} \times T^{4.2526} \times \exp(-2117.7702/T)$	for secondary carbon sites
	$k(T) = 7.27607 \times 10^{-26} \times T^{4.1476} \times \exp(-1743.4889/T)$	for tertiary carbon sites

If the BHG barrier heights and average values for other factors are used, the rate constants are denoted by RC-TST/BHG. The RC-TST/BHG rate constants for any reactions belonging to this class can be estimated without any further calculations as:

$$k(T) = 2.1369 \times 10^{-26} \times T^{4.4983} \times \exp\left(\frac{-2613.9911}{T}\right) (\text{cm}^3\ \text{s}^{-1}\ \text{molecule}^{-1})$$

for primary carbon sites (13a)

$$k(T) = 7.74811 \times 10^{-26} \times T^{4.2526} \times \exp\left(\frac{-2117.7702}{T}\right) (\text{cm}^3\ \text{s}^{-1}\ \text{molecule}^{-1})$$

for secondary carbon sites (13b)

$$k(T) = 7.27607 \times 10^{-26} \times T^{4.1476} \times \exp\left(\frac{-1743.4889}{T}\right) (\text{cm}^3\ \text{s}^{-1}\ \text{molecule}^{-1})$$

for tertiary carbon sites (13c)

The appropriate symmetry factors of three for primary carbon sites, two for secondary, and one for tertiary carbon site are included in the rate constant expressions above. Correction for the number of equivalent H abstraction site depends on specific reactant and thus must be included explicitly.

3.5. Error Analyses. As mentioned earlier, only a limited amount of the experimental data is available for the hydrogen abstraction by the vinyl radical reaction class. H abstractions from primary (reaction R_2) and secondary (reaction R_3) carbon atoms in propane are used to illustrate the theory. It is noted that there is no direct experimental data available for these reactions. The literature data available come from either BEBO calculations[25] or extensive literature review.[26] Figure 7a,b shows the predicted rate constant of reactions R_2 and R_3 using the RC-TST method and from literature data.[25,26] In this figure, the "RC-TST LER" notation means that the reaction class factors were calculated with the approximate expressions listed in Table 6. Because there are not big differences between the results obtained from either using the BH&HLYP/cc-pVDZ or AM1 reaction energies, only rate constants from BH&HLYP are presented here. The agreement between the predicted results and data derived by Tsang for both reactions is excellent in the high-temperature regime ($T > 800$ K). For the temperatures lower than 800 K, the differences are more noticeable.

The second error analysis compares RC-TST results with those from explicit calculations. Such a comparison between the calculated rate constants for a small number of reactions using both the RC-TST and the full TST/Eckart methods

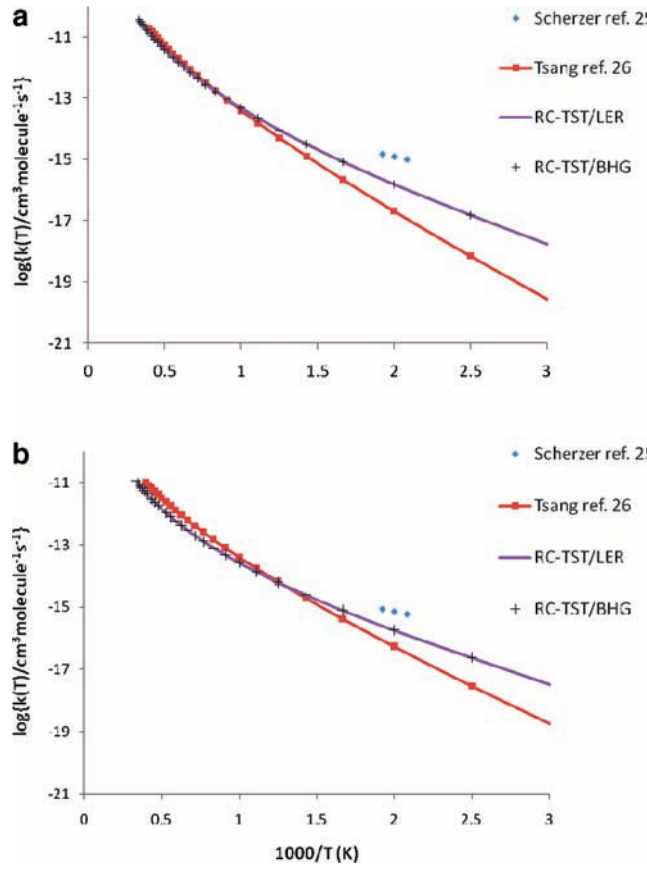

Figure 7. Arrhenius plots of the calculated and literature rate constants using the RC-TST methods for the $CH_3CH_2CH_3 + C_2H_3 \rightarrow CH_2{\cdot}CH_2CH_3 + C_2H_4$ and $CH_3CH_2CH_3 + C_2H_3 \rightarrow CH_3CH_2{\cdot}CH_3 + C_2H_4$ reactions. Results from using the reaction energies at the BH&HLYP/cc-pVDZ level in the LER are presented.

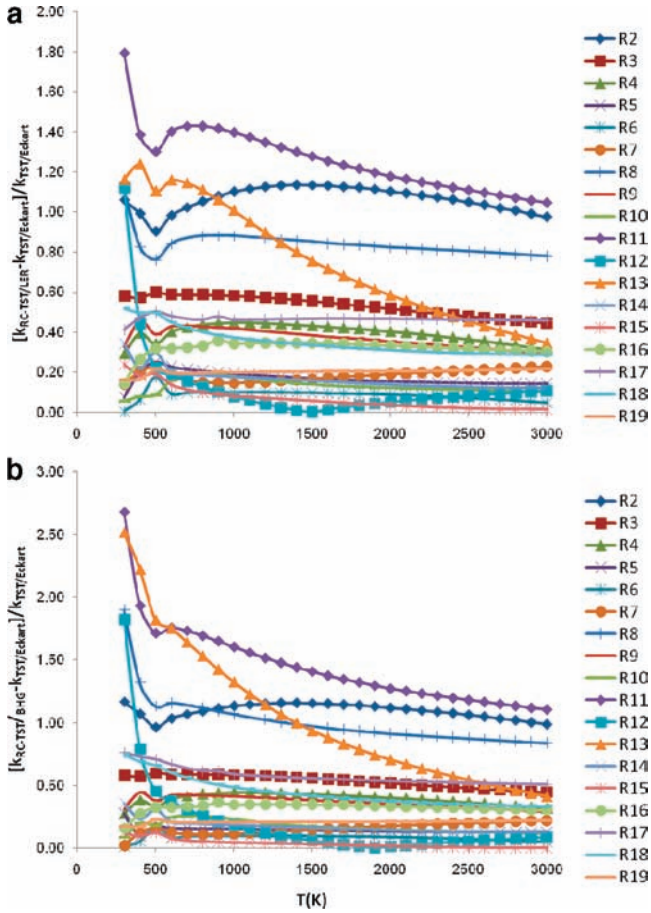

Figure 8. Relative absolute deviations as functions of the temperature between rate constants calculated from explicit TST/Eckart calculations for all selected reactions and (a) from the RC-TST/LER method where BH&HLYP reaction energies were used for the LER and (b) from the RCT-TST/BHG method.

provides additional information on the accuracy of the RC-TST method. To be consistent, the TST/Eckart rate constants of the reference reaction were used in calculation of RC-TST rate constants for this particular analysis rather than using the expression in eq 7. The results for this error analysis for 18 representative reactions (i.e., the comparisons between the RC-TST/LER and full TST/Eckart methods) are shown in Figure 8a, wherein the relative deviation defined by ($|k^{\mathrm{TST/Eckart}} - k^{\mathrm{RC\text{-}TST/LER}}|/k^{\mathrm{TST/Eckart}}$) as a percent vs the temperature for all reactions in the representative set, R_2-R_{19} is plotted. For the temperatures >500 K, most of the reactions in this set, 14 out of 18, the unsigned relative errors are within 60%. In the low temperatures regime, five reactions have errors larger than 60%. So, in general, it can be concluded that RC-TST can estimate thermal rate constants for reactions in this class within 60% when compared to those calculated explicitly using the TST/Eckart method. For other cases, except for R11, the maximum error is less than 120%, which is still an acceptable level of accuracy for reaction engineering purposes. It is noted that this analysis is presented for the RC-TST/LER only. One would expect the performance for the RC-TST/BHG approach is slightly worse that those of RC-TST/LER as shown in Figure 8b, wherein the maximum error, for two reactions, exceeds 200%. Thirteen of 18 reactions are within the 70% error limits in all temperature ranges, however. As expected, these differences are only minor.

Finally, an analysis on the systematic errors in different factors in the RC-TST/LER methods was performed. These

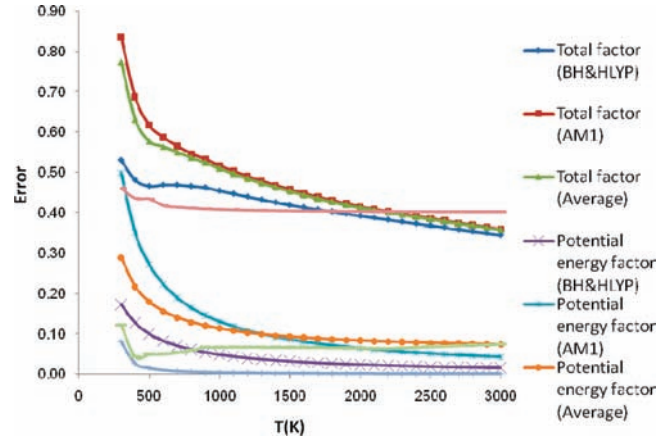

Figure 9. Averaged absolute errors of the total relative rate factors $f(T)$ (eq 2) and its components, namely, the tunneling (f_K), partition function (f_Q), and potential energy (f_V) factors as functions of temperature.

errors are from the use of fitted analytical expressions for the potential energy factor, tunneling factor, and partition function factor introduced in the method. The deviations/errors between the approximated and exact factors within the TST framework are calculated at each temperature for every reaction in the representative set and then averaged over the whole class. For the LER approach, error in the potential energy factor comes from the use of the LER expression: that of the tunneling factor, from using three equations (eqs 9a−c); that of the partition function factor, from using eqs 10a−c; and that of the HR factor from using eq 11. Absolute errors averaged over all 18 reactions, R_2-R_{19}, as functions of the temperature are plotted in Figure 9. Of the factors, the HR and partition function ratios factor show the least temperature dependence for the whole temperature range. The tunneling factor introduced the smallest error of less than 10% in the low temperature regime and almost equal to 0 for $T > 800$ K. The error from the partition function factor is largest for $T > 300$ K, about 40% for the whole temperature range. The error from the AM1 LER potential energy factor decreases from 50% at 300 K as the temperature increases. The error of the BH&HLYP LER potential energy factor is smaller than 20%, whereas BHG shows an error not larger than 30%. Thus, the BH&HLYP LER approach gives less error in the potential energy factor than the BHG. The AM1 method yields the worst performance for this reaction class. For $T > 1500$ K, the errors from both the LER and the BHG factors are almost the same. For temperature range $T > 1000$ K, all of the errors are almost constant. For most cases, the total systematic errors due to the use of simple analytical expressions for different reaction class factors are less than 60% for the temperature range 300−3000 K. For the AM1 LER and BHG approaches, these errors are larger but not to exceed 90%.

In general, if accurate rate constants needed, the BH&HLYP RC-TST/LER is recommended, while the BHG approach gives a quick estimation without doing any quantum chemistry calculation but with larger errors.

4. Conclusion

The application of the RC-TST combined with the LER (RC-TST/LER) and the BHG (RC-TST/BHG) approach to predict thermal rate constants of the hydrogen abstraction by vinyl radical from alkanes reaction class was carried out. The literature value of the rate constants for the reference $C_2H_3 + C_2H_6 \rightarrow C_2H_4 + C_2H_5$ reaction was used. All necessary parameters for

predicting rate constants of any reaction in this class were derived from a set of representative reactions. The error analyses indicate that the RC-TST/LER method can predict rate constants within a factor of 2 as compared to explicit rate calculations. The performance for the RC-TST/BHG method is slightly worse. However, the convenience of ready to be used rate expressions for any reaction in the class would offset the less accuracy of the BHG approach as compared to that of the LER.

Acknowledgment. We thank the computational center in Warsaw (ICM) for providing access to the supercomputer resources and the Gaussian 03 program (Grant G33-03).

References and Notes

(1) Colket, M.; Edwards, T.; Williams, S.; Cernansky, N. P.; Miller, D. L.; Egolfopoulos, F.; Lindstedt, P.; Seshadri, K.; Dryer, F. L.; Law, C. K.; Friend, D.; Lenhert, D. B.; Pitsch, H.; Sarofim, A.; Smooke, M.; Tsang, W. American Institute of Aeronautics and Astronautics 2008.

(2) D'Anna, A.; Violi, A.; D'Alessio, A. *Combust. Flame* **2000**, *121*, 418.

(3) Hansen, N.; Kasper, T.; Klippenstein, S. J.; Westmoreland, P. R.; Law, M. E.; Taatjes, C. A.; Kohse-Hoinghaus, K.; Wang, J.; Cool, T. A. *J. Phys. Chem. A* **2007**, *111*, 4081.

(4) Pope, C. J.; Miller, J. A. *Proc. Combust. Inst.* **2000**, *28*, 1519.

(5) Frenklach, M.; Clary, D. W.; Gardiner, W. C.; Stein, S. E. *Proc. Combust. Inst.* **1985**, *25*, 887.

(6) Miller, J. A.; Klippenstein, S. J.; Robertson, S. H. *J. Phys. Chem.* **2000**, *104*, 7525.

(7) Striebel, F.; Jusinski, L. E.; Fahr, A.; Halpern, J.; Klippenstein, S.; Taatjes, C. A. *Phys. Chem. Chem. Phys.* **2004**, *6*, 2216.

(8) D'Anna, A.; D'Alessio, A.; Kent, J. *Combust. Flame* **2001**, *125*, 1196.

(9) Zhang, S.; Truong, T. N. *J. Phys. Chem. A* **2003**, *107*, 1138.

(10) Kungwan, N.; Truong, T. N. *J. Phys. Chem. A* **2006**, *109*, 7742.

(11) Huynh, L. K.; Panasewicz, S.; Ratkiewicz, A.; Truong, T. N. *J. Phys. Chem.* **2007**, *111*, 2156.

(12) Huynh, L. K.; Ratkiewicz, A.; Truong, T. N. *J. Phys. Chem. A* **2006**, *110*, 473.

(13) Bankiewicz, B.; Huynh, L. K.; Ratkiewicz, A.; Truong, T. N. *J. Phys. Chem. A* **2009**, *113*, 1564.

(14) Truong, T. N. *J. Chem. Phys.* **2000**, *113*, 4957.

(15) Frisch, M. J.; Trucks, G. W.; Schlegel, H. B.; Scuseria, G. E.; Robb, M. A.; Cheeseman, J. R.; Montgomery, J. A., Jr.; Vreven, T.; Kudin, K. N.; Burant, J. C.; Millam, J. M.; Iyengar, S. S.; Tomasi, J.; Barone, V.; Mennucci, B.; Cossi, M.; Scalmani, G.; Rega, N.; Petersson, G. A.; Nakatsuji, H.; Hada, M.; Ehara, M.; Toyota, K.; Fukuda, R.; Hasegawa, J.; Ishida, M.; Nakajima, T.; Honda, Y.; Kitao, O.; Nakai, H.; Klene, M.; Li, X.; Knox, J. E.; Hratchian, H. P.; Cross, J. B.; Adamo, C.; Jaramillo, J.; Gomperts, R.; Stratmann, R. E.; Yazyev, O.; Austin, A. J.; Cammi, R.; Pomelli, C.; Ochterski, J. W.; Ayala, P. Y.; Morokuma, K.; Voth, G. A.; Salvador, P.; Dannenberg, J. J.; Zakrzewski, V. G.; Dapprich, S.; Daniels, A. D.; Strain, M. C.; Farkas, O.; Malick, D. K.; Rabuck, A. D.; Raghavachari, K.; Foresman, J. B.; Ortiz, J. V.; Cui, Q.; Baboul, A. G.; Clifford, S.; Cioslowski, J.; Stefanov, B. B.; Liu, G.; Liashenko, A.; Piskorz, P.; Komaromi, I.; Martin, R. L.; Fox, D. J.; Keith, T.; Al-Laham, M. A.; Peng, C. Y.; Nanayakkara, A.; Challacombe, M.; Gill, P. M. W.; Johnson, B.; Chen, W.; Wong, M. W.; Gonzalez, C.; Pople, J. A. *Gaussian 03*, Revision A.1; Gaussian, Inc.: Pittsburgh, PA, 2003.

(16) Becke, A. D. *J. Chem. Phys.* **1993**, *98*, 1372.

(17) Lee, C.; Yang, W.; Parr, R. G. *Phys. Rev.* **1988**, *37*, 785.

(18) Truong, T. N.; Duncan, W. *J. Chem. Phys.* **1994**, *101*, 7408.

(19) Lynch, B. J.; Fast, P. L.; Harris, M.; Truhlar, D. G. *J. Phys. Chem. A* **2000**, *104*, 4811.

(20) Truong, T. N. http://CSE-Online.net.

(21) Ayala, P. Y.; Schlegel, H. B. *J. Chem. Phys.* **1998**, *108*, 2314.

(22) Huynh, L. K.; Zhang, S.; Truong, T. N. *Combust. Flame* **2008**, *152*, 177.

(23) Petty, J. T.; Harrison, J. A.; Moore, C. B. *J. Phys. Chem.* **1993**, *97*, 11194.

(24) Hidaka, Y.; Shiba, S.; Takuma, H.; Suga, M. *Int. J. Chem. Kinet.* **1985**, *17*, 441.

(25) Scherzer, K.; Loser, U.; Stiller, W. *Z. Chem.* **1987**, *27*, 300.

(26) Tsang, W.; Hampson, R. F. *J. Phys. Chem. Ref. Data* **1986**, *15*, 1087.

(27) Liu, G.; Li, Z.; Xiao, J.; Liu, J.; Fu, Q.; Huang, X.; Sun, C.; Tang, A. *ChemPhysChem* **2002**, *7*, 625.

JP903762X